

## Electron-excited $3d$ hole states of $\text{La}^{3+}$ in solids

P. Motais, E. Belin, and C. Bonnelle

*Laboratoire de Chimie Physique (Laboratoire associé au Centre National de la Recherche Scientifique No. 176),  
Université Pierre et Marie Curie, 11 rue Pierre et Marie Curie, F-75231 Paris Cédex 05, France*

(Received 2 March 1984)

The  $\text{La}^{3+}$  excited states with a  $3d$  inner hole are investigated by x-ray absorption spectroscopy (XAS), electron-stimulated x-ray emission spectroscopy (EXES), and characteristic isochromat spectroscopy (CIS). The relative energies of these various states are determined and their decay processes are considered. It is shown that the levels associated with the  $\text{La}^{3+} 3d^9 4f^1$  configuration are well described in  $jj$  coupling. It is shown that the  $3d^9 4f^1$  configuration states decay by direct recombination of the excited electron and the inner hole and simultaneously by transitions taking place in the presence of the extra  $4f$  electron. The emissions already observed by Liefeld *et al.* close to the  $3d_{3/2}$  and  $3d_{5/2}$  thresholds are studied and interpreted as  $f$ - $d$  discrete emissions from  $J$  levels of the  $3d^9 4f^2$  configuration. A nonradiative transition from  $J$  levels of this same configuration is also evidenced by CIS at the  $3d_{3/2}$  threshold; it is identified as a  $3d_{3/2}^{-1} 4f^2 \rightarrow 3d_{5/2}^{-1} 4f^1$  Coster-Kronig-type process. The various nonradiative processes transferring a  $3d_{3/2}$  hole to a  $3d_{5/2}$  hole are considered and their relative intensity discussed. From all of the results it is concluded that final-state-type coupling effects are weak in the radiative decay of  $3d^{-1}$  excited states in  $\text{La}^{3+}$ .

### I. INTRODUCTION

Electron-stimulated x-ray emission spectroscopy (EXES) is a method of investigating the properties of states with a hole in a core level (x-ray states) created by the electron bombardment. In solids the x-ray states are usually ionization states, the inner electron being ejected into the continuum. In some cases excited x-ray states may also be present with a lifetime sufficiently long for their radiative decay to be observable. As an example, it is now well known that the emission lines observed in the  $3d$  spectra of lanthanides in coincidence with each absorption line, and called resonance lines ( $R$  lines), are due to the inverse process of absorption, i.e., to the direct radiative deexcitation of the  $3d^9 4f^{m+1}$  monoexcited states to the ground state.<sup>1-3</sup> As previously emphasized,<sup>4</sup> the presence of intense resonant emissions in the spectrum of a solid shows that the excited electron has a high probability of remaining localized on the same atom with the same spin during the lifetime of the inner hole, and that the interaction between the excited state and the conduction states remains weak. One expects that such excited x-ray states must be described in terms of a quasiatomic model, but very little is actually known of the properties of these states. In particular, an important point is to determine if the  $3d^9 4f^{m+1}$  excitation states are formed directly by collisional interaction between the incident electron and the core electron, or if their formation results from a two-step process: step 1 being ionization and step 2 involving a relaxation process with stabilization of the  $4f$  shell.<sup>5,6</sup> We shall show that the data deduced from x-ray photoemission spectroscopy (XPS) and x-ray emission and absorption spectra can resolve this point.

In a system having strongly localized empty states, emissions other than the  $R$  lines can also be observed as a consequence of the electron-beam excitation. In fact, a

systematic study of the La and Ce  $3d$ -emission spectra by Liefeld *et al.*<sup>7,8</sup> as a function of the incident-electron energy  $E_0$  showed, for  $E_0$  close to the  $3d_{5/2}$  and  $3d_{3/2}$  thresholds, the presence of features located below each main emission line. They were ascribed to a resonance in the bremsstrahlung radiation. Since then, various theoretical studies and other interpretations have been proposed for these emissions.<sup>9-16</sup> We have suggested<sup>13</sup> that they are resonant lines in an excited system having a trapped slow electron, and we designate them  $R^e$  lines.

Here, we present an analysis of the La  $3d$ -emission spectrum in two trivalent compounds,  $\text{LaF}_3$  and  $\text{La}_2\text{O}_3$ , with the aim of studying the various excited x-ray states created in the lanthanides under electron irradiation. These results are compared with the metal. It is known that the La  $3d$ - $4f$  photoexcitation spectrum is simple, offering essentially two intense well-resolved transitions.<sup>17</sup> In the same way, since no  $f$  electrons are present in the La ground state, the  $3d$ -emission spectrum is less complex than that of other lanthanides.<sup>18</sup> It makes La convenient for a detailed analysis of electron-stimulated excited x-ray states. La in metallic form has received particular attention: the position of the empty  $4f$  level has been determined by continuum-limit spectroscopy<sup>7</sup> and bremsstrahlung isochromat spectroscopy (BIS);<sup>7,19</sup> the dependence of the energy of the  $4f$  level on the electron configuration has been studied by various appearance potential spectroscopies (APS) and characteristic-electron-energy-loss spectroscopy.<sup>12,20</sup>

To identify the various precursor states of each x-ray emission in the La  $3d$  spectrum between 800 and 870 eV, and to deduce the various decay processes of these precursor states, we have (i) analyzed the La  $3d$  emission spectrum, compared to the photoabsorption, for several values of the incident-electron energy,  $E_0$ , from threshold to several times the threshold value, and (ii) performed the

isochromats of each emission observable over this range. We show for the first time that in the case of  $\text{LaF}_3$  and  $\text{La}_2\text{O}_3$  each of these emissions takes place from a *discrete excited state*. We then deduce new information on the  $R^e$  lines and the decay processes of electron-stimulated excited x-ray states in lanthanum for the metal and wide-gap insulating compounds.

In Sec. II we give a brief description of the experimental procedure. A concise analysis of present data on the electronic structure of lanthanum in  $\text{LaF}_3$ ,  $\text{La}_2\text{O}_3$ , and the metal is given in Sec. III. In Sec. IV we report our results concerning the  $3d^9 4f^1$  excited states as deduced from resonant emissions and photoabsorption. The other lines present in the  $\text{La } 3d$ -emission spectra are considered in Sec. V. In Sec. VI the bremsstrahlung and characteristic isochromat spectra are presented. Data deduced from these spectra on the formation of  $3d^9 4f^1$  and  $3d^9 4f^2$  states and their radiative and nonradiative decay are discussed in Sec. VII. The conclusions are presented in Sec. VIII.

## II. EXPERIMENTAL PROCEDURE

$\text{LaF}_3$  and  $\text{La}_2\text{O}_3$  samples were prepared by vacuum deposition on appropriate clean substrates at room temperature at a residual pressure of about  $10^{-6}$  Torr. For  $\text{LaF}_3$ , spectroscopically pure powdered fluoride was used; for  $\text{La}_2\text{O}_3$ , spectroscopically pure La was evaporated and oxidized after deposition under pure dry oxygen. For the x-ray emissions copper targets were used on which the fluoride and oxide depositions were made. The absorption screens were thin layers  $\sim 100$ – $1000$  Å thick deposited onto Al ( $0.5 \mu\text{m}$ ) or Makrofol ( $2 \mu\text{m}$ ) substrates.

The spectra were analyzed by means of a 50-cm-radius bent crystal vacuum spectrometer equipped with mica or beryl slabs, and using a polypropylene-windowed  $\text{Ar-CH}_4$  gas-flow proportional counter placed behind an adjustable slit situated on the Rowland circle. The spectral resolving power available was about  $10^4$ .

The absorption spectra were recorded using the bremsstrahlung radiation emitted by a W target bombarded by electrons of 1400 eV energy. The x-ray characteristic emissions were produced by means of an electron beam and analyzed perpendicular to it. Two types of emission spectra have been recorded: (i) one type obtained by varying the Bragg angle at a given energy of the incident electrons (standard x-ray emission), and (ii) one type obtained by keeping the Bragg angle constant and varying the energy of the incident electrons by steps of 0.65 eV (characteristic isochromat spectroscopy i.e., CIS).

In CIS only  $\text{LaF}_3$  targets were studied, as the fluoride is particularly stable and not as sensitive as the oxide to surface contamination, especially by water vapor.<sup>21</sup> Owing to the voltage across the x-ray-source filament, the energy resolving power was about  $10^3$ .

Let us note that to obtain the isochromat of a given x-ray line, it is necessary to take into account the contributions from neighboring x-ray lines because a possible overlap between their energy distributions may occur. To do this, we have fitted calculated curves to the emission lines

and subtracted the contribution due to the closest lines; thus corrected intensity curves are obtained.

## III. ELECTRONIC STRUCTURE

$\text{La}$  trifluoride is a wide-gap insulator: The  $\text{F}^- 2p$  levels form the valence band, and  $\text{La } 5d$  and  $6s$  levels, slightly mixed with  $\text{F}^- 3s$ , form the conduction band. The optical properties of  $\text{LaF}_3$  in the vacuum-ultraviolet region have already been investigated and compared to those of the early rare-earth trifluorides,  $\text{CeF}_3$ ,  $\text{PrF}_3$ , and  $\text{NdF}_3$ .<sup>22</sup> It was shown that in these three compounds the  $4f$  levels are present in the band gap and are not mixed with the valence band. This is in agreement with the x-ray photoemission spectrum of  $\text{CeF}_3$ , according to which the  $\text{Ce } 4f$  level lies about 5 eV above the valence band.<sup>23</sup> Moreover, no  $4f$  electron is present in  $\text{LaF}_3$ .

When a  $3d$  hole is created in a rare-earth ion, a modification of the electronic distribution is expected. According to the equivalent-core approximation, one approximates the  $Z$  element with an inner hole to the  $Z+1$  element. Thus by analogy with the  $\text{Ce}$  compounds one expects that a normally empty  $4f$  excitation level is present in the band gap of  $\text{LaF}_3$  several electron volts above the valence band. A  $3d$  electron has a high probability to be excited to this empty  $4f$  level, and the  $3d^9 4f^1$  state can thus be formed by a direct excitation process. The ground state of the  $3d^9$  ion, on the other hand, has the  $3d^9 4f^0$  configuration, and the formation of the excited ion with a hole in the valence band,  $3d^9 V^{-1} 4f^1$ , requires energy. This explains the presence of high-binding-energy satellites in the  $\text{La } 3d$  photoemission of  $\text{LaF}_3$ .<sup>24</sup> These satellites are due to charge transfer from the valence band to the empty  $4f$  level by a shakeup process simultaneously with the creation of a  $3d$  inner hole.

For the sesquioxides one expects the electronic configuration to be similar. But in this case the valence band arises from the  $\text{O}^{2-} 2p$  levels and the valence-band to  $4f$ -level energy separation is about half that of the trifluorides. However, in the presence of a  $3d$  hole, the empty  $\text{La } 4f$  excitation level still lies above the valence band. In an atomic model the  $3d^9 V^{-1} 4f^1$  configuration is an excited configuration of the  $3d^9 4f^0$  nonexcited configuration ion, and a charge transfer from the top of the valence band to the  $4f$  level requires energy. Then the  $3d^9 4f^1$  excited state is obtained by direct excitation of a  $3d$  electron to the empty  $4f$  level. A similar behavior is expected for other compounds of lanthanum but not for all of them; in fact, in some  $\text{Ce}$  compounds the  $4f$  level lies very close to the valence band and it is difficult to foresee what the ground configuration of the  $3d^9 \text{La}$  ion will be.

In  $\text{La}$  metal the empty  $4f$  level is pulled down 1.8 eV below the Fermi energy by the  $3d$  hole<sup>20</sup> and it can be filled by an electron from the valence band with a stabilization of energy. Indeed, Creelius *et al.*<sup>5</sup> have observed a low-binding-energy satellite in the  $3d$  XPS of  $\text{La}$  metal 3.2 eV below each main  $3d$  peak with an intensity of only 5–6% of that of the main peak. The formation of the  $3d^9 4f^1$  excited state by ionization and relaxation is thus possible, but hardly probable, and the excited state is

essentially formed by a direct process. In Ref. 5 it has been suggested that the binding energy of the  $3d_{5/2}$  low-energy satellite (832.4 eV) is related to that of the  $3d_{5/2}$  absorption, but the value of Fisher and Baun,<sup>25</sup> which corresponds to the low-energy inflexion point of the principal absorption line was used. Indeed, because the relaxation process is not governed by dipole-selection rules, the binding energy of the satellite must be compared to the baricenter of various  $J$  levels associated to the  $3d_{5/2}^{-1}4f^1$  configuration. The agreement is satisfactory between the experimental value and our calculated value of 831.8 eV (see Sec. IV A). On the other hand, the  $3d_{5/2}$  principal peak-satellite separation corresponds to the difference between the energies of the  $3d^9 4f^0$  and  $3d^9 4f^1$  configurations.

Hence we deduce that the excited  $4f$  level associated with the  $3d^9 4f^1$  configuration can tunnel into the extended states in the metal, whereas this type of interaction is not possible in  $\text{LaF}_3$  and  $\text{La}_2\text{O}_3$  because the  $4f$  level is situated in the band gap. The study of  $\text{La } 3d^9 4f^1$  excited states in these three materials allows us to determine which are the solid-state effects due to this interaction.

#### IV. RESONANT EMISSIONS AND $3d$ ABSORPTION LINES

##### A. Energies

Two intense emission lines are observed in the  $\text{La } 3d$  spectrum in coincidence with the two principal  $3d$  photoabsorption lines (Fig. 1); they are identified as resonant emissions. Their position is independent of the material considered to within the experimental precision,  $\pm 0.1$  eV. Since the  $\text{La } 3d$ - $4f$  emission and absorption lines are positioned at the same energy in the metal and the two compounds, we confirm that the interactions between the excited  $4f$  level and the extended states, possible only in the metal, must remain weak and the  $3d^9 4f^1$  state retains strong atomic character in the solid.

These results are in agreement with the well-known fact that the  $3d$  photoabsorption of the solid lanthanides is described by atomic transitions of the type  $3d^{10} 4f^N \rightarrow 3d^9 4f^{N+1}$ .<sup>26,17,27</sup> As opposed to the  $4d$  case, where the exchange interaction is the largest, in the  $3d$  photoabsorption case, the  $3d$  spin-orbit interaction is larger than the electrostatic interactions, where the exchange integral  $G^1$

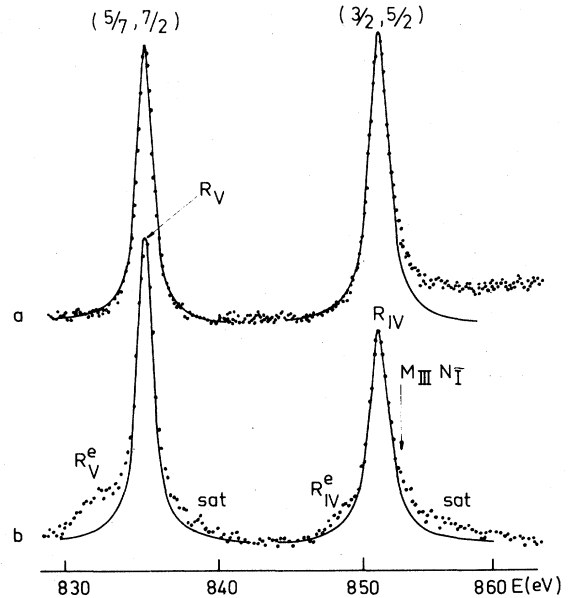


FIG. 1.  $\text{La } 3d$  spectra in  $\text{La}_2\text{O}_3$ . (a) Photoabsorption; (b) emission at 1.2 keV. Dots denote experimental data, solid line denotes Lorentzian curve.

is even smaller than the direct one  $F^2$ . Thus the structure of the  $\text{La}^{3+} 3d^9 4f^1$  configuration is essentially determined by the  $3d$  spin-orbit-coupling parameter, and the term dependence, which is known to be large in the presence of a strong exchange interaction,<sup>28</sup> is not significant here.

With this in mind, we have performed a calculation in intermediate coupling followed by a recoupling transformation from  $L$ - $S$  to  $jj$ . The parameters used are given in Table I, together with the percentage compositions of the levels. It appears that the purity is high in  $jj$  coupling, as previously found for  $\text{Tm}^{3+} 3d$  photoabsorption.<sup>29</sup> As a consequence, we designate the excited states  $3d^9 4f^1$  in this coupling. In contrast, in the  $4d$  photoabsorption the percentage of  $jj$ -coupling states is low and the levels have almost pure  $L$ - $S$ -coupling character. Thus for the strong peak, a 99.8%  $^1P_1$  ( $L$ - $S$ ) character is predicted, while its  $(\frac{3}{2}, \frac{5}{2})$  ( $jj$ ) character is only about 45%.<sup>30</sup> This large difference between the  $3d$ - $4f$  and  $4d$ - $4f$  electrostatic

TABLE I. Calculated baricenter and excitation energies for the  $\text{La } 3d^9 4f^1$  configuration. The percentage compositions are shown for the three radiative levels. The radial parameters are also given.

Energies (eV)		jj-coupling percentage		L-S-coupling percentage
Average	Excitation			
831.8	830.3	88.7% $d_{5/2}f_{5/2}$ + 11.1% $d_{5/2}f_{7/2}$		76.7% $^3P$ + 23.0% $^3D$
	834.6	84.5% $d_{5/2}f_{7/2}$ + 11.3% $d_{5/2}f_{5/2}$		49.5% $^3D$ + 38.8% $^1P$
848.5	850.9	95.6% $d_{3/2}f_{5/2}$		60.9% $^1P$ + 27.5% $^3D$
Parameters (meV)				
$F^2 = 5.985$ , $F^4 = 2.633$ , $G^1 = 3.990$ , $G^3 = 2.237$				
$G^5 = 1.525$ , $\zeta_d = 6.650$ , $\zeta_f = 80$ ,				
				$p_A = p \frac{d_{5/2}f_{7/2}}{d_{3/2}f_{5/2}} = 0.63$

and spin-orbit interactions means that the spectral characteristics of  $3d$  photoabsorption differ from those observed for the  $4d$  photoabsorption.<sup>31</sup>

In addition, we have determined the energy of 20  $J$  levels belonging to the  $3d^9 4f^1$  configuration and the barycenters of the  $3d_{5/2}^{-1} 4f^1$  and  $3d_{3/2}^{-1} 4f^1$  configurations (cf. Table I). These are situated  $-2.8$  and  $-2.4$  eV below the  $(\frac{5}{2}, \frac{7}{2})$  and  $(\frac{3}{2}, \frac{5}{2})$  radiatively decaying states, respectively, which are the highest-lying states in each  $3d_{5/2}$  or  $3d_{3/2}$  range.

Unlike  $3d$  photoemission,  $3d$  photoabsorption is identical for the three materials. In fact, the photoabsorption is very strongly dominated by the excitation to the discrete states and, in this process, the  $4f$  excited electron partially screens the core hole. The photoemission describes the ionization and is very sensitive to perturbations which accompany the formation of the  $3d$  hole, that is to say, essentially sensitive to shake up processes involving the valence electrons.

### B. Shape and width

Once the contributions from the other emissions have been removed, we find that the two resonant emissions can be fitted by Lorentzian curves for both the metal and the compounds. In the case of  $\text{La}_2\text{O}_3$  irradiated under 1 keV, the full widths at half maximum (FWHM's) of the  $(\frac{5}{2}, \frac{7}{2})$  and  $(\frac{3}{2}, \frac{5}{2})$  emissions are 1.2 and 1.8 eV, respectively. As is well known, a resonant emission of Lorentzian shape is characteristic of the decay of a discrete atomic state which falls exponentially with a lifetime of  $\hbar/\text{FWHM}$ . Then, one also expects the photoexcitation lines which correspond to the transitions from the ground state to these same states to be Lorentz curves.

Indeed, the  $(\frac{5}{2}, \frac{7}{2})$  absorption line is a Lorentzian curve of the same FWHM as the  $(\frac{5}{2}, \frac{7}{2})$  resonant emission. The  $(\frac{3}{2}, \frac{5}{2})$  absorption transition can be fitted by the superposition of a Lorentz curve of the same FWHM as the  $(\frac{3}{2}, \frac{5}{2})$  resonant emission in addition to an arctangent curve; the latter curve has the same width as the  $(\frac{3}{2}, \frac{5}{2})$  line, has a low amplitude, and is situated on the high-energy side of the  $(\frac{3}{2}, \frac{5}{2})$  maximum at a distance of about  $+2.2$  eV in the case of the  $\text{La}_2\text{O}_3$ .

This shows that a weak absorption jump is present at the  $3d_{3/2}$  threshold. A very faint jump is also observed at the  $3d_{5/2}$  threshold when the contrast is increased by the use of a thick sample (Fig. 2); under these conditions the absorption jump at  $3d_{3/2}$  is strongly enhanced and clearly identifiable by the presence of a distinct elbow in the curve. Moreover, the lines are broadened, the  $(\frac{5}{2}, \frac{5}{2})$  transition becomes observable, and the cross section decreases beyond the  $3d_{3/2}$  threshold as expected in the case of one-particle behavior. Thus the direct ionization process is present in the  $3d$  photoabsorption, whereas it is not revealed in the  $4d$  photoabsorption. From the ratio between the amplitude of the  $(\frac{3}{2}, \frac{5}{2})$  line and the  $3d_{3/2}$  absorption jump we have estimated the probability for direct ionization at the  $3d_{3/2}$  threshold to be approximately 9% of that of the direct excitation. Since the  $3d_{5/2}$  jump is much lower than the  $3d_{3/2}$  one, one can deduce that ioni-

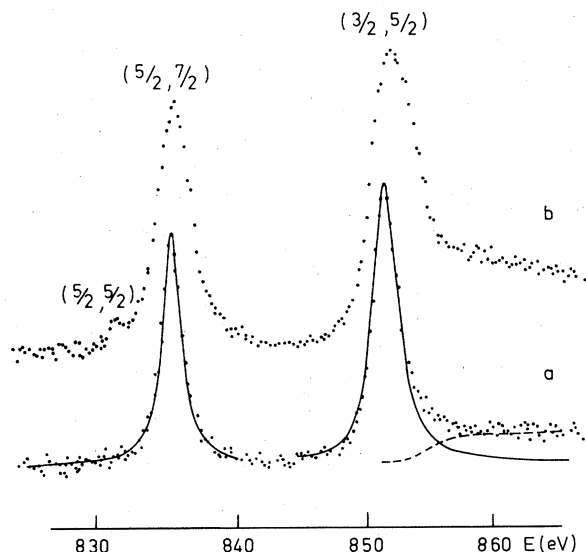


FIG. 2. La  $3d$  photoabsorption in  $\text{La}_2\text{O}_3$  for two sample thicknesses: (a) 280 Å; (b) 1350 Å. Dots denote experimental data, solid line denotes Lorentzian curve, and dashed line denotes arctangent curve.

zation takes place essentially towards the  $4f$  continuum with  $\frac{5}{2}$  character. On the other hand, as already mentioned,<sup>32</sup> the  $3d_{3/2}$  ionization energy is relatively close to the sum of  $(\frac{5}{2}, \frac{7}{2})$  excitation and  $5p$  ionization energies. This concordance can perhaps enhance the transitions to continuum states beyond the  $3d_{3/2}$  threshold.

The absorption and resonant emission lines have thus the same Lorentzian shape and the same width to within the experimental precision. We return to this point in the discussion.

### C. Intensity

The relative intensities of the absorption lines have been calculated in the same manner as described in Ref. 27. With the parameters indicated in Table I, the predicted intensity ratio for the transitions to the  $(\frac{5}{2}, \frac{7}{2})$  and  $(\frac{3}{2}, \frac{5}{2})$  states is 0.63, in agreement with the ratio  $\rho_A$  of areas measured under the two corresponding absorption lines ( $\rho_A=0.61$  for  $\text{La}_2\text{O}_3$ ).<sup>32</sup> The transition to the  $(\frac{5}{2}, \frac{5}{2})$  state is predicted to be only 1% of the one to the  $(\frac{5}{2}, \frac{7}{2})$  state (Fig. 2). Thus only two intense resonance lines are expected in the emission spectrum, in agreement with the experiment (Fig. 1).

The ratio  $\rho_E$  of the areas measured under the resonant emissions of Fig. 1 [ $\rho_E=(\frac{5}{2}, \frac{7}{2})/(\frac{3}{2}, \frac{5}{2})=0.95$ ] is clearly higher than the ratio  $\rho_A$  of absorption lines. We had suggested that this result was due to the existence of discrete nonradiative transitions of Coster-Kronig type taking place between the  $J=1$  level with a  $3d_{3/2}$  hole and the  $\text{La}^{4+}$  ion with a  $3d_{5/2}$  hole.<sup>32</sup> Indeed, such decay processes are in competition with the  $(\frac{3}{2}, \frac{5}{2})$  resonant emission and can contribute to decrease its intensity. We shall show that other processes can modify  $\rho_E$ .

The evaluation of  $\rho_E$  is more difficult than that of  $\rho_A$  and the  $5p_{1/2}-3d_{3/2}$  characteristic line is superimposed on the  $(\frac{5}{2}, \frac{7}{2})$   $R$  line in the metal (cf. Sec. V A). Nevertheless, we can assume that  $\rho_E$  has the same value in the three materials. Consequently, in this paragraph we neglect possible solid-state effects and assume the resonant emissions are transitions taking place between discrete states of the  $3d^9 4f^1$  excited configuration and the  $3d^{10} 4f^0$  ground state.

The intensity of a resonant emission cannot be described by the simple model given in Ref. 33. Indeed, the excitation and radiative-decay probabilities as well as the self-absorption must be taken into account. We have seen that the  $3d^9 4f^1$  state is produced essentially by direct collisional excitation, a stabilization of the  $4f$  shell in the  $3d^9$  ion being also possible in the case of the metal. In the latter process, the twelve  $J$  levels of the  $3d_{5/2}^{-1} 4f^1$  configuration can be excited with a probability which depends on the statistical weight of each  $J$  level. Then the probability that the  $J=1$  ( $\frac{5}{2}, \frac{7}{2}$ ) level will be excited is only 3.5% of the probability of the corresponding twelve  $J$  levels. The value is 5.5% for the  $J=1$  ( $\frac{3}{2}, \frac{5}{2}$ ) level. Its contribution to the formation of resonant emission precursor states is thus very small.

In what follows we consider only the collisional excitation: In the range of validity of the Bethe-Born approximation, i.e., for  $E_0$  more than twice the threshold, the optically allowed excitations predominate to a great degree, and the collisional excitation can be written as a function of the optical oscillator strength. In this approximation the intensity of an electron-stimulated resonant emission is proportional to<sup>4</sup>

$$h\nu \left[ \frac{W_s}{\sum_i W_i} \right] \frac{\sigma_{\text{ph}}}{h\nu} \int_0^b \frac{1}{E} \ln(aE) e^{-\sigma_T N y_x} dx, \quad (1)$$

where  $E$  is the incident-electron energy at a depth  $x$ ,  $h\nu$  is the energy of the resonant emission,  $W_s$  is the probability of the direct radiative deexcitation, the  $W_i$  are the various deexcitation probabilities,  $\sum_i W_i$  is proportional to the width of the excited state,  $\Gamma$ ,  $\sigma_{\text{ph}}$  is the photoexcitation cross section corresponding to the line of energy  $h\nu$ ,  $a$  is a function of the momentum change supported by the incident electron during the collision,  $e^{-\sigma_T N y_x}$  is the self-absorption term,  $\sigma_T$  is the total absorption cross section which can be approximated by  $\sigma_{\text{ph}}$  at the resonance,  $y_x$  is the path of the x-ray radiation in the target in the direction of observation corresponding to a range  $x$  for the incident electrons, and  $N$  is the number of atoms per unit volume. The integration is taken over the effective path length of the incident electron in the target, i.e., to a depth  $b$  where the average energy of the electron has fallen to the excitation-energy threshold.<sup>34</sup>

We have calculated<sup>35</sup> the intensity ratio  $\rho_E$  for various values of  $E_0$  between the  $3d_{3/2}$  threshold and 5 keV by means of relation (1), the method set out in Ref. 34, and the stopping law of Feldman.<sup>36</sup> The values of  $\sigma_{\text{ph}}$  are deduced from the photoabsorption spectrum. The statistical weights of two precursor states ( $J=1$ ) being the same, the ratio of direct radiative deexcitation probabilities of the two states is equal to the ratio of their  $\sigma_{\text{ph}}$  cross sections.

The widths  $\Gamma$  are the FWHM's measured for each excitation line. For large values of  $E_0$ , the self-absorption is large and the corresponding term tends to a value proportional to  $1/\sigma_{\text{ph}}$ . Then  $\rho_E$  tends to

$$\left[ \frac{W_s}{\sum_i W_i} \right]_{3d_{5/2}} / \left[ \frac{W_s}{\sum_i W_i} \right]_{3d_{3/2}} \equiv \frac{(\sigma_{\text{ph}})_{d_{5/2}} \Gamma_{3/2}}{(\sigma_{\text{ph}})_{d_{3/2}} \Gamma_{5/2}},$$

i.e., 0.94, in agreement with the experimental results.  $\rho_E$  is only slightly larger than  $\rho_A$ , however, when  $E_0 \sim 200$  eV above the  $3d$  thresholds. It is expected to vary between the two extremes as  $E_0$  varies between 1.1 and 3 keV.

The emission spectra are plotted in Fig. 3 for various energies  $E_0$  between 0.85 and 5 keV. Whatever  $E_0$ , the  $(\frac{5}{2}, \frac{7}{2})$  and  $(\frac{3}{2}, \frac{5}{2})$  resonant emissions coincide with the absorption lines. This confirms that the intensity of these emissions is governed by the dipole-selection rules and only the  $J=1$  levels of the  $3d^9 4f^1$  configuration participate in these transitions. The measurement of  $\rho_E$  is possible only after unfolding the emission spectra into their various components. The error introduced is difficult to estimate. Whatever the value of  $E_0$ , for  $\rho_E$  we obtain an experimental value which is larger than the calculated one. The difference is of the order of probable errors beyond about 2.2 keV, i.e., in the range where the Bethe-Born approximation is valid. This agreement shows that over this range the electron-excitation cross sections are well governed by the optical oscillator strengths.

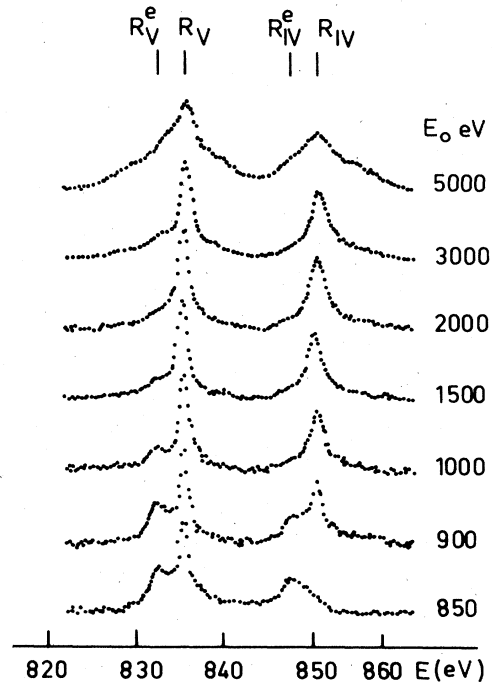


FIG. 3. La  $3d$  emissions in  $\text{La}_2\text{O}_3$  observed for various incident electron energies  $E_0$ .

On the other hand, near the threshold the difference between the experimental and calculated values exceeds the probable error and the experimental values do not follow the same variation with  $E_0$  as the calculated ones. As is well known, over this range the generalized oscillator strength cannot be assimilated to the optical oscillator strength, and relation (1) is no longer valid. In fact, all the  $J$  levels of the  $3d^9 4f^1$  configuration can be excited. According to our results the ratio of electron-excitation cross sections to the  $J=1$  levels should be close to unity. No data for the electron-excitation cross section of inner shells near their threshold are available for comparison.

Consequently, the increase in  $\rho_E$  with respect to  $\rho_A$  is due, to a very large extent, to the processes which made the ratio  $\Gamma_{3/2}/\Gamma_{5/2}$  larger than unity, in agreement with the preceding results.<sup>32,33</sup> However, we shall see in Sec. VI that other processes not contributing to the widths of  $3d^9 4f^1$  excited states can create the precursor state of the  $(\frac{5}{2}, \frac{7}{2})$  resonant emission. Such processes modify  $\rho_E$  differently according to  $E_0$  and contribute to make the values of  $\rho_E$  larger than the predicted ones close to threshold.

Independently, two important points must be emphasized concerning the absolute intensity of the resonant emissions: First, we have verified that its variation with  $E_0$  is different from that of characteristic x-ray emissions.<sup>4</sup> This confirms that the precursor state of the  $R$  lines is not formed by ionization followed by relaxation. Second, the intensity is slightly weaker in the metal than in  $\text{LaF}_3$  and  $\text{La}_2\text{O}_3$ . We interpret this difference as a solid-state effect; it is discussed in Sec. VII A.

## V. OTHER EMISSION LINES

Apart from the intense resonance lines, three other types of lines are present in the  $\text{La } 3d$ -emission spectrum.

### A. Lines due to transitions between normally filled levels

The  $3p_{3/2}-4s$  and  $3d_{3/2,5/2}-5p_{1/2,3/2}$  atomic transitions are located in the spectral range we have considered. The energies of these transitions for La in metal,  $\text{LaF}_3$ , and  $\text{La}_2\text{O}_3$  have been calculated from the photoemission binding energies (cf. Table II). The  $3p_{3/2}-4s$  line ( $M_{III}-N_1$ ) is very close to the  $R_{IV}$  emission on the high-transition-energy side; it is mixed with the satellites and, consequently, cannot be resolved. The same is expected for the  $3d_{3/2}-5p_{1/2,3/2}$  lines, the calculated energies of which are very close to those of the intense emission  $R_V$ . Only the  $3d_{5/2}-5p_{3/2}$  emission can be resolved.

For La metal we observe an emission at 819.0 eV, in agreement with the calculated value for the  $3d_{5/2}-5p_{3/2}$  transition; its intensity is only a few percent of that of  $R_V$ . Another emission of larger intensity is present at 812.4 eV, i.e., shifted by 6.6 eV toward lower energies with respect to the first line. For  $\text{La}_2\text{O}_3$  and  $\text{LaF}_3$ , no line is observed at the expected position; a single emission is present at 812.4 eV, coincident with the low-energy emission of the metal (Fig. 4).

Similar behavior is observed for the  $3d_{5/2}-5p_{3/2}$  emis-

TABLE II. Energies of the levels from available photoemission measurements and expected and observed x-ray emission energies (all in eV).

	Energies of the levels (eV)			
	La	$\text{La}_2\text{O}_3$		
$5p_{3/2}$	16.8 <sup>a</sup>	18.8 <sup>b</sup>		
$5p_{1/2}$	19.3 <sup>a</sup>	21.3 <sup>b</sup>		
$4s$	270 <sup>c</sup>			
$3d_{5/2}$	832.4 <sup>d</sup>			
	835.6 <sup>d</sup>	837.7 <sup>e</sup> 841.6 <sup>e</sup>		
$3d_{3/2}$	852.4 <sup>a</sup>	854.5 <sup>e</sup> 858.4 <sup>e</sup>		
$3p_{3/2}$	1123 <sup>e</sup>			
	X-ray emission energies (eV)			
	La		$\text{La}_2\text{O}_3$	
	Expected	Observed	Expected	Observed
$5p_{3/2}-3d_{5/2}$	818.8	812.4 819.0	818.9	812.4
$5p_{1/2}-3d_{3/2}$	833.1	828.6	833.2	828.6
$4s-3p_{1/2}$	853			
$R_V$		834.9		834.9
$R_{IV}$		851.5		851.5

<sup>a</sup>Reference 37. <sup>b</sup>Reference 39. <sup>c</sup>Reference 38. <sup>d</sup>Reference 5. <sup>e</sup>Reference 24.

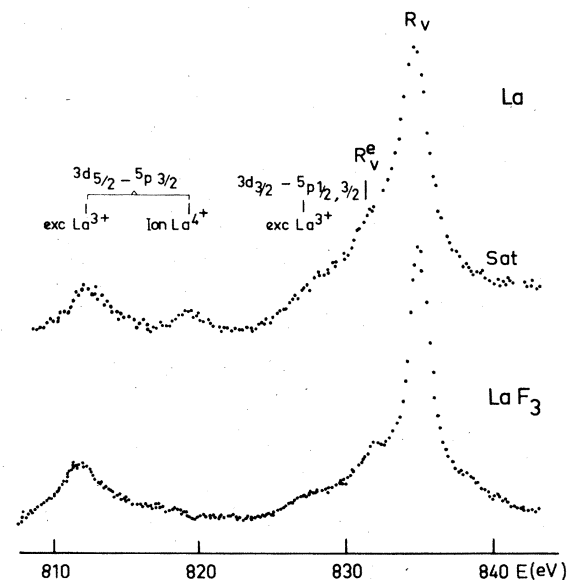


FIG. 4. Comparison of  $\text{La } 3d$  emissions in the metal and in  $\text{LaF}_3$  observed at  $E_0=2.8$  keV.

sions of Gd and Tb metal and oxide. It has been interpreted<sup>40</sup> as a modification of the electronic distribution in the oxide subsequent to the formation of the inner hole: A valence electron should be localized in a  $4f$  orbital to screen the charge due to the  $3d$  hole, the final configuration being  $3d^9 4f^{m+1} V^{-1}$ . However, in the  $\text{Gd}_2\text{O}_3$   $3d$  photoemission spectrum,<sup>41</sup> no peak is present to make such an interpretation possible. The same thing is true for  $\text{La}_2\text{O}_3$  and  $\text{LaF}_3$ . In fact, the  $\text{La } 3d_{3/2}$  and  $3d_{5/2}$  core-level satellite peaks characteristic of the  $3d^9 4f^1 V^{-1}$  configuration lie at a higher binding energy than that of the principal peak, and from them the energy of the  $3d_{5/2}-5p_{3/2}$  line should be 823 eV. Moreover, no peak is seen in the photoemission spectrum of  $\text{La}_2\text{O}_3$  and  $\text{LaF}_3$  toward the lower-binding-energy side of the  $3d$  principal peaks. Then, it is not possible to explain the low-transition-energy x-ray emission observed for  $\text{LaF}_3$  and  $\text{La}_2\text{O}_3$  from photoemission spectra, i.e., from the energies of the levels.

We suggest that this low-energy emission corresponds to the  $3d_{5/2}-5p_{3/2}$  transition in the excited configuration  $3d_{5/2}^{-1} 4f^1$ . Indeed, the energy of the  $3d_{5/2}-5p_{3/2}$  transition is expected to be smaller in the presence of an extra  $4f$  electron than in the  $3d^9$  ion: For this estimate the energy of the initial state is taken to be equal to the average energy of all the  $J$  levels of the  $3d_{5/2}^{-1} 4f^1$  configuration, i.e., 831.8 eV (cf. Table I); it is approximately 4–5 eV smaller than the energy of the  $3d$  level. On the other hand, the  $5p$  electrons are repelled by the  $4f$  electron. Then the energy of the  $3d_{5/2}-5p_{3/2}$  transition is smaller in the excited configuration than in the ionized one, in agreement with the observed shift.

By considering that the transitions to  $3d_{3/2}$  shift in the same manner, we identify the weak line present at about 828.6 eV in the spectra of  $\text{LaF}_3$  and  $\text{La}_2\text{O}_3$  to be the unresolved  $3d_{3/2}-5p_{1/2,3/2}$  emissions in the excited system. This line is also weaker in the metal than in the compound.

Hence, for  $\text{LaF}_3$  and  $\text{La}_2\text{O}_3$  the  $3d_{5/2}-5p_{3/2}$  transition is observed only in the excited configuration and not in the  $3d_{5/2}^{-1}$  ion. We deduce from this that the number of  $3d_{5/2}^{-1}$  ions created in the experimental conditions of Fig. 4 is very small with respect to the number of the  $3d_{5/2}^{-1} 4f^1$  states. Likewise, the number of  $3d_{5/2}^{-1}$  ions formed by an autoionization process from the excited states must be very small. It has previously been suggested<sup>33,42</sup> that the increase in width of the  $(\frac{3}{2}, \frac{5}{2})$  emission (there denoted  $^1P$ ) with respect to the  $(\frac{5}{2}, \frac{7}{2})$  emission ( $^3D$ ) is due mainly to the process  $3d_{3/2}^{-1} 4f^1 \rightarrow 3d_{5/2}^{-1}$ . If we suppose that the widths associated with the autoionization and the other processes are additive, the increase would have to be explained by the autoionization of a third of the  $3d_{3/2}^{-1} 4f^1$  states initially formed. The number of  $3d_{5/2}^{-1}$  ions would then be approximately half the number of  $3d_{5/2}^{-1} 4f^1$  ( $\frac{5}{2}, \frac{7}{2}$ ) excited states. Then the  $3d_{5/2}-5p_{3/2}$  emission could be observed in the  $3d_{5/2}^{-1}$  ion, contrary to our observations. In fact, other processes can contribute to broaden the  $3d_{3/2}^{-1} 4f^1$  ( $\frac{3}{2}, \frac{5}{2}$ ) level with respect to the  $3d_{5/2}^{-1} 4f^1$  ( $\frac{5}{2}, \frac{7}{2}$ ) level. A large number of states can be formed with an energy excess of about 16 eV corresponding to the  $3d_{3/2}-3d_{5/2}$  difference if the valence states and all the  $J$  levels of the excited configuration are considered (cf. Sec. VI C).

For the metal, the  $3d_{5/2}-5p_{3/2}$  line is observed simultaneously in the two configurations. We interpret the difference between the metal and the compounds by a solid-state effect; this is discussed in Sec. VII A.

### B. Satellite emissions

Satellite emissions are observed on the high-transition-energy side of the resonance lines; they correspond to transitions in multiply excited or excited-ionized systems. These lines are not resolved in the two compounds and are spread over about 5–6 eV. Their intensity is very weak; it increases slightly with  $E_0$  and they are clearly observable only beyond 3 keV.

As generally observed, the satellite lines are clearly more intense in the metal than in the compounds because the multiple excitation by shakeup process is more probable in a conductor than in a wide-gap insulator. Thus, in the metal a distinctly resolved feature is seen at about +6 eV of each resonant emission. These lines are difficult to interpret because various states with similar energies can be created concurrently and only precise calculations can make their interpretation possible.

### C. $R^e$ lines

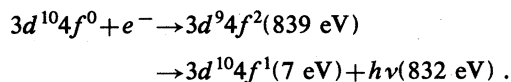
Two  $R^e$  lines are present about 3 eV below each  $R$  line. Their intensity varies very strongly as a function of  $E_0$ : In fact, these lines are very intense for a value of  $E_0$  just above the excitation threshold, and then their intensity decreases rapidly as  $E_0$  increases; however, they are still observed for energies equal to several times the threshold (cf. Fig. 3).

The  $R^e$  lines were seen for the first time by Liefeld *et al.*<sup>7,8</sup> from experiments made close to  $3d$  thresholds and interpreted as a resonance in the bremsstrahlung radiation. These results have been confirmed by various authors.<sup>9,11</sup> A many-body model was developed to explain these observations.<sup>10</sup> Subsequently, other studies have been made and have led to different interpretations. Thus an alternative explanation in terms of a one-electron model has been proposed by Kanski *et al.*<sup>12</sup> from experiments of electron-excited Auger-electron APS, electron-stimulated x-ray APS and characteristic-electron-energy-loss spectroscopy. On the other hand, from the CIS of La metal obtained by Riehle,<sup>43</sup> Ulmer<sup>14</sup> has interpreted the  $R^e_V$  line as a radiative transition of an electron of the valence band to the  $3d_{5/2}$  core hole. Kanski and Wendin<sup>15</sup> proposed that the  $R^e$  lines were due to the decay of a  $3d^9 V^{-1} 4f^2$  state formed by shakeup excitation. Recently, it has been suggested that these features should arise from multiplet effects of the  $3d^9 4f^1$  configuration.<sup>16</sup>

We have suggested<sup>13</sup> that the  $R^e$  lines should be ascribed to radiative transitions from discrete states created by collisional interaction between the incident electron and the atom. During the single excitation by impact of an electron whose energy just exceeds the core-hole excitation threshold, a complex state consisting of two excited electrons in the hole field can be formed. Indeed, if a projectile electron is slowed down to such an extent that, after exciting the  $3d^9 4f^1$  state, its velocity becomes comparable

to that of the excited electron, the two electrons remain correlated until a dissociation process of the complex takes place. Such a complex has the  $3d^9 4f^2$  configuration; its formation has already been suggested by various authors.<sup>7-12</sup> As emphasized by Liefeld *et al.*,<sup>7</sup> projectile electrons having an energy just equal to that necessary for the  $3d^9 4f^2$  configuration to be created will always be present whatever their initial energy  $E_0$ . This is due to the collisional slowing down of incident electrons in the material, and explains that the  $R^e$  lines can be observed whatever  $E_0$  is.

Then, by analogy with the process of resonant emission, we have suggested that the  $R^e$  lines are due to the direct radiative deexcitation of states of the  $3d^9 4f^2$  configuration, i.e., to transitions



It must be noted that in agreement with this interpretation the separation between the  $R^e$  and  $R$  lines is of the same order of magnitude as the separation between the more intense  $3d$  photoabsorption lines of Ce III and Ce IV which correspond to the transitions  $3d^{10}4f^1 \rightarrow 3d^9 4f^2$  and  $3d^{10} \rightarrow 3d^9 4f^1$ , respectively. This interpretation will be discussed again in Sec. VII B by taking into account the results that we deduce from the CIS of  $R$  and  $R^e$  lines.

## VI. ISOCHROMAT SPECTRA

### A. Bremsstrahlung isochromat

A bremsstrahlung isochromat spectrum (BIS), obtained for  $\text{LaF}_3$  at about 860 eV, i.e., away from any characteristic x-ray transition, is shown in Fig. 5(a). It describes the scattering of incident electrons into the empty conduction levels of the system at the ground state and gives the distribution of these levels. Its shape is comparable to that of the BIS obtained for metallic lanthanum.<sup>7,44</sup> By analo-

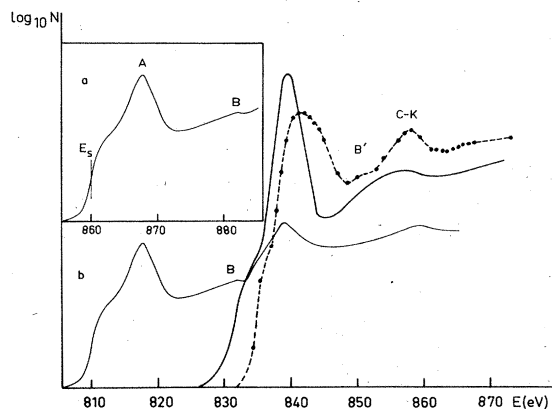


FIG. 5. Logarithmic curves of La isochromats in  $\text{LaF}_3$ . (a) Bremsstrahlung isochromat, (b) characteristic isochromats. Dashed line denotes  $R_V$  line, solid line denotes  $R_V^e$  line, and dashed-dotted line denotes  $3d_{5/2}-5p_{3/2}$  line.

gy with the proposed interpretation for La, we ascribe the increase in intensity at the threshold ( $E_s \sim h\nu$ ) to the lowest empty conduction states and the strong peak ( $A$ ) to  $4f$  empty levels; these are situated 6.9 eV above the bottom of the conduction band in  $\text{LaF}_3$ , instead of 5.5 eV in the metal. A feature labeled  $B$  is seen about 15 eV above the threshold; it involves the presence of a maximum in the empty-state distribution; a density-of-states calculation would be necessary to determine the character of these states.

### B. Characteristic isochromats in the range $3d_{5/2}$

The characteristic isochromat spectra, or excitation functions, of lines  $R_V$ ,  $R_V^e$ , and  $3d_{5/2}-5p_{3/2}$  are plotted in Figs. 5(b) and 6 for  $\text{LaF}_3$ . Figure 5(b) corresponds to raw experimental data with a logarithmic intensity scale. In Fig. 6 each spectrum with a linear scale is corrected by taking into account the overlap of the closest transitions, i.e.,  $R_V^e$  and  $3d_{3/2}-5p$  for  $R_V$ ,  $R_V$  and  $3d_{3/2}-5p$  for  $R_V^e$  (cf. Sec. II). The results obtained for  $\text{La}_2\text{O}_3$  are similar.

Usually, a CIS describes the inelastic scattering of incident electrons in the empty conduction levels accompanied by the excitation of an atomic  $nl$  electron in the same levels. Therefore, at the threshold of an x-ray characteristic emission, two electrons are present in the first empty levels, the incident electron and the electron ejected from an atomic inner shell. If the perturbations due to the presence of the inner hole can be neglected, the CIS corresponds to the self-convolution of the empty-state distribution as obtained by BIS. None of the three CIS of Fig. 5(b) corresponds to such a curve.

In the case where a resonant emission is stimulated by direct collisional excitation, the ejected electron is localized in a discrete excited level and only the incident electron is free to move in the empty conduction states. The CIS is thus a function of two terms: the probability that the excited level will be formed, and the empty-state distribution in the excited system. Moreover, because the threshold energy and the emitted-photon energy  $h\nu_R$  are the same, BIS and  $R$  CIS are superimposed.

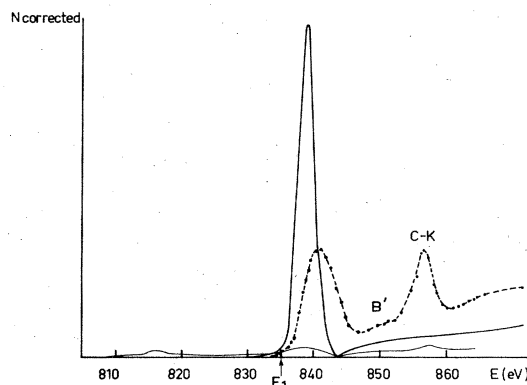


FIG. 6. La  $3d_{5/2}$  characteristic isochromats for  $\text{LaF}_3$ . Dashed line denotes  $R_V$  line, thick solid line denotes  $R_V^e$  line, and thin solid line denotes  $3d_{5/2}-5p_{3/2}$  line.

Let us consider the  $R_V$  CIS [Fig. 5(b) and 6]. Only the  $(\frac{5}{2}, \frac{7}{2})$  level of the  $3d^9 4f^1$  excited configuration contributes to the  $R_V$  emission. As expected, the observed threshold energy ( $E_1$ ) is equal to the energy of this level and the intensity increases rapidly just above the threshold. An asymmetrical enlarged maximum is observed 5.5 eV above  $E_1$ . Towards the higher incident-electron energies the intensity decreases more gradually, then increases again; several features of unequal intensity are present. The first feature, labeled  $B'$ , is located about 15 eV above the threshold and corresponds to feature  $B$  in the BIS spectra. The intense feature labeled CK (Coster-Kronig) is close to the  $3d_{3/2}$  threshold. This peak and the one accompanying it at higher energies will be discussed in Sec. VIC.

The isochromat spectrum observed at the energy of the  $3d_{5/2}-5p_{3/2}$  line (812.4 eV) is much less intense than the  $R_V$  CIS. At the threshold ( $E_s \sim h\nu$ ), the spectrum is identical to the BIS because only the continuum radiation is excited. The excitation threshold of the  $3d_{5/2}-5p_{3/2}$  line is shifted down by about 2 eV with respect to the  $R_V$  line. This shift confirms that, firstly, for  $\text{LaF}_3$  and  $\text{La}_2\text{O}_3$ , the  $3d_{5/2}-5p_{3/2}$  emission is observed in the system of  $3d^9 4f^1$  configuration and not in the ion of larger ionization energy; secondly, at threshold the excitation by electrons is not governed by optical selection rules, and all the  $J$  levels of the excited configuration participate in the  $3d-5p$  transitions. On the other hand, the shape of the maximum is not exactly the same as that of the  $R_V$  CIS. However, the superposition of the BIS in the case of  $R_V$  can explain, in part, the broadening observed on the high-energy side in  $R_V$  and not in the  $3d_{5/2}-5p_{3/2}$  CIS. A feature is also seen near the  $3d_{3/2}$  threshold at the same energy in the  $3d_{5/2}-5p_{3/2}$  and  $R_V$  CIS, showing that the two CIS are similar.

The shape of the  $R_V^e$  CIS is very different from that of the  $R_V$  CIS: We observe, from the threshold energy which is equal to the energy of the  $R_V^e$  line,  $h\nu(R_V^e)$ , an increase in intensity equivalent to that of BIS, and then an intense almost symmetrical peak (FWHM of 2.8 eV from Fig. 6) at about 839 eV, i.e., approximately 4 eV above the  $3d^9 4f^1$  excitation threshold; this maximum is clearly more intense than the  $R_V$  maximum (Fig. 6). Toward higher energies the intensity again falls to the value of the BIS before a faint monotonic increase takes place which makes it more intense than the BIS; no feature is observed in this region. By taking into account the instrumental broadening, it appears that the energy range in which the  $R_V^e$  line is emitted intensely is narrowly determined; it is less than 2 eV wide. The small extent of the  $R_V^e$  CIS maximum with respect to that of the  $R_V$  CIS and the absence of density-of-states features beyond the maximum suggest that, in a narrow energy range centered on the maximum of the  $R_V^e$  CIS, the system formed by  $\text{La}^{3+}$  and the incident electron is in a discrete state. As a consequence, we deduce that over a range of less than 2 eV centered on 839 eV, the incident electron has a strong probability of being scattered in a localized atomic  $4f$  state, together with a second  $4f$  electron excited from the atomic  $3d$  level by making the configuration of the system to be  $3d_{5/2}^{-1} 4f^2$ . Then in the  $R_V^e$  initial state, the incident electron is localized on the excited  $\text{La}^{3+}$  ion and no electron is

free to move in the empty states, in contrast with the  $R_V$  initial state where the incident electron is decoupled from the excited  $\text{La}^{3+}$  ion and moves in the potential of this ion and of the neighboring ions. In this model, the law of energy conservation imposes that only the incident electrons having energies equal to the energies of radiative  $J$  levels of the  $3d_{5/2}^{-1} 4f^2$  configuration participate in the transition  $3d_{5/2}^{-1} 4f^2 \rightarrow 3d^{10} 4f^1 + h\nu$ . The  $R_V^e$  CIS thus represents the probability that these levels can be created under electron impact as a function of electron-beam energy  $E_0$ . This probability is at a maximum when  $E_0$  is just equal to the energy of radiative levels having the  $3d_{5/2}^{-1} 4f^2$  configuration. The increase in the CIS intensity beyond the maximum corresponds to the proportion of incident electrons having an energy in this range.

From the position of the  $R_V^e$  CIS maximum, we deduce that the average energy of the  $3d_{5/2}^{-1} 4f^2$  configuration radiative states exceeds the  $3d^9 4f^1$  ( $\frac{5}{2}, \frac{7}{2}$ ) excitation energy by 4 eV (cf. Fig. 6). By taking into account the separation between the  $R_V$  and  $R_V^e$  lines, which is

$$\begin{aligned} h\nu(R_V) - h\nu(R_V^e) \\ = E(3d^9 4f^1 - 3d^{10} 4f^0) - E(3d^9 4f^2 - 3d^{10} 4f^1), \\ \sim +3 \text{ eV}, \end{aligned}$$

and the energy of  $3d^{10} 4f^1$  as deduced from the BIS, one obtains

$$E(3d^9 4f^2 - 3d^9 4f^1) \sim 4 \text{ eV},$$

in qualitative agreement with the value deduced directly from Fig. 6. This difference involves only the  $J$  levels participating in the  $R_V$  and  $R_V^e$  radiative transitions. According to Table I, the separation between the  $(\frac{5}{2}, \frac{7}{2})$  level and the baricenter of the  $3d^9 4f^1$  configuration is 2.8 eV. A separation of the same sign equal to 2.4 eV has been found between the radiative levels and the baricenter of the  $3d^9 4f^2$  configuration in  $\text{Ce}^{3+}$ .<sup>45</sup> Then it is possible to deduce that the average energy of the  $3d^9 4f^2$  configuration exceeds that of  $3d^9 4f^1$  by approximately 4 eV. Let us note that, from Ref. 20, the  $3d^9 4f^2 - 3d^9 4f^1$  separation would be only 1.6 eV in the metal, but this value is obtained from various spectroscopies taking into account other  $J$  levels for the two configurations.

The  $3d^9 4f^2 - 3d^9 4f^1$  separation is the energy necessary for the incident electron to surmount the potential barrier and to be localized in a discrete level; it gives a measurement of the  $f-f$  Coulomb repulsion energy.

On the other hand, the maximum of the  $R_V^e$  CIS is below the principal part of the  $R_V$  CIS. One deduces from this result that the potential energy necessary to create the discrete state  $3d_{5/2}^{-1} 4f^2$  is smaller than that of the  $3d_{5/2}^{-1} 4f^1 \epsilon f^1$  state. Therefore the energies of various states can be arranged in the following order:

$$E[3d^9 4f^1(\frac{5}{2}, \frac{7}{2})] < E(3d_{5/2}^{-1} 4f^2) < E[3d^9 4f^1(\frac{5}{2}, \frac{7}{2}) \epsilon f^1].$$

It must be emphasized that, in BIS and  $R_V^e$  CIS, the separation between the threshold and the maximum,  $\Delta E$ , is the same:

$$\Delta E(R_V^e \text{ CIS}) = 3d_{5/2}^{-1}4f^2 - h\nu(R_V^e) = 3d^{10}4f^1 - 3d^{10} \\ = \Delta E(\text{BIS}).$$

The intermediate state  $3d_{5/2}^{-1}4f^2$  relaxes via photon emission in a final state identical to that of the bremsstrahlung process.

We have seen that the  $R_V$  CIS describes the inelastic scattering of the incident electron into an empty electron level accompanied by the excitation of an atomic  $3d$  electron into a localized  $4f$  level. Because the spectrum is identical for  $\text{LaF}_3$  and  $\text{La}_2\text{O}_3$ , we suggest that the incident electron is preferentially scattered into an  $f$  level. When the scattering of the incident electron takes place in such a level, the final state of the resonant-emission process is  $3d^{10}4f^1$ , i.e., the same as that of the  $R_V^e$  line and bremsstrahlung process.

### C. Characteristic isochromats in the $3d_{3/2}$ region

The CK feature observed close to the  $3d_{3/2}$  threshold in the  $R_V$  and  $3d_{5/2}-5p_{3/2}$  CIS reveals the possibility for a system with a  $3d_{3/2}$  hole to decay very rapidly to a system with the  $3d_{5/2}^{-1}4f^1$  configuration. Various processes can transfer a  $3d_{3/2}$  hole to a  $3d_{5/2}$  hole; they are shown schematically in Fig. 7. Among them only the processes leading to the precursor state of the  $R_V$  line need be taken into account to explain the CK feature.

Firstly, we consider the transition denoted I in Fig. 7. All the  $J$  levels of the  $3d_{3/2}^{-1}4f^2$  initial configuration can contribute to the  $3d_{3/2}^{-1}4f^2-3d_{5/2}^{-1}4f^1$  nonradiative transition. Then one expects a feature in the  $R_V$  CIS 2–3 eV below the peak of the  $R_V^e$  CIS, in agreement with our observations. We label transition I a Coster-Kronig-type transition. Its probability must be relatively large at the threshold because the Coster-Kronig  $3d_{3/2}-3d_{5/2}$   $X$  transitions are the most probable amongst the nonradiative transitions expected in lanthanide ions with a  $3d_{3/2}$  hole.<sup>46</sup> Moreover, its contribution can explain the slight enhancement of  $R_V$  CIS beyond the  $3d_{3/2}$  threshold. In

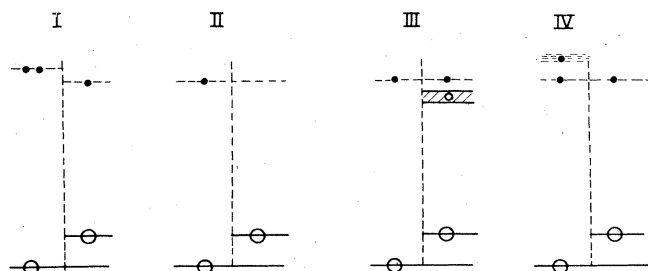


FIG. 7. Schematic representation of possible  $3d_{3/2}^{-1}3d_{5/2}^{-1}$  transitions for lanthanum. I denotes  $3d_{3/2}^{-1}4f^2 \rightarrow 3d_{5/2}^{-1}4f^1$ , II denotes  $3d_{5/2}^{-1}4f^1 \rightarrow 3d_{5/2}^{-1}$ , III denotes  $3d_{3/2}^{-1}4f^1 \rightarrow 3d_{5/2}^{-1}4f^1V^{-1}$ , and IV denotes  $3d_{5/2}^{-1}4f^1 + 1e^- \rightarrow 3d_{5/2}^{-1}4f^1$ .

fact, as seen from the  $R_V^e$  CIS, the formation of  $3d_{3/2}^{-1}4f^2$  is possible whatever the energy of incident electrons. Process I contributes to increase the width of the  $R_V^e$  line and to decrease its intensity. On the other hand, it does not modify the  $R_{IV}$  line, but enhances the intensity of the  $R_V$  line above the  $3d_{3/2}$  threshold, in agreement with our observation.

The equivalent process from the  $3d_{3/2}^{-1}4f^1$  configuration (denoted II in Fig. 7) leads to the  $3d_{5/2}^{-1}$  ion. It does not contribute to the feature present in the  $R_V$  CIS and does not modify the  $R_V$  line. On the other hand, it increases the width of the  $R_{IV}$  line and decreases its intensity. We have seen that this process is not very probable because in the compounds no  $3d-5p$  transition is observed in the  $3d_{5/2}^{-1}$  ion, and for the metal this transition is weak.

The  $3d_{3/2}-3d_{5/2}$  separation being about 16 eV, only another Coster-Kronig-type transition is possible from the  $3d_{3/2}^{-1}4f^1$  configuration; it is denoted III in Fig. 7. Its final state,  $3d_{5/2}^{-1}4f^1V^{-1}$ , can decay via emission of a  $R_V$  satellite. However, all the  $J$  levels of the initial and final configurations can contribute to process III, and the participation of the  $3d-4f$  radiative transitions to the total decay of this excited state is weak. Process III is possible whatever the incident-electron energy. It increases the width and decreases the intensity of the  $R_{IV}$  line. It leaves  $R_V$  invariant except if the energy separation between  $R_V$  and the satellite is sufficiently small for the two lines not to be resolved.

Lastly, a process could be considered at the threshold (process IV): the incident electron would participate in this process and would be localized in the presence of the  $3d_{5/2}^{-1}$  final hole. Process IV is less probable than process I. It increases the width and decreases the intensity of  $R_{IV}$ ; it increases the intensity of  $R_V$ . However, as it is possible only at the threshold, it cannot explain the results observed for the higher energies of incident-electron beam.

In summary, the CK feature observed in the  $R_V$  CIS is due to process I and, to a lesser extent, to process IV. These processes contribute to enhance the intensity of the  $R_V$  line with respect to that of  $R_{IV}$  at the  $3d_{3/2}$  threshold and beyond. Moreover, process I is responsible for the broadening of the  $R_V^e$  line with respect to that of the  $R_V$  line and its relatively weak intensity. The width of the  $R_{IV}$  line and its decrease in intensity are due essentially to process III and, to some extent, to process II. It is surprising that process III should be more probable than process II. Nevertheless, this can be explained from the high stability of the  $3d_{5/2}^{-1}4f$  configuration which makes a transition to  $3d_{5/2}^{-1}4fV^{-1}$  more probable than to the  $3d_{5/2}^{-1}$  ion.

## VII. DISCUSSION

### A. $3d^94f^1$ states

Various properties of the  $3d^94f^1$  configuration states can be deduced from our experimental results. In the first place, some important points must be emphasized.

(a) Contrary to what is expected according to various authors,<sup>6</sup> the  $3d^94f^1$  states are created only by direct col-

lisional excitation in  $\text{La}_2\text{O}_3$  and  $\text{LaF}_3$ . The same is probably true for other lanthanum insulating compounds. In the metal, the direct excitation is largely predominant and the contribution of the relaxation process to the formation of the  $J=1$  levels can be neglected. On the other hand, the relaxation process can contribute weakly to the excitation of other  $J$  levels of the  $3d^9 4f^1$  configuration.

(b) The observation of  $5p$ - $3d$  characteristic emissions in excited  $\text{La}^{3+}$  with a spectator  $4f$  electron shows that the decay of the  $\text{La}^{3+} 3d^9 4f^1$  states can take place through atomic processes other than the direct recombination of the excited electron and the inner hole. This confirms that the resonant emissions are not of an excitonic type.<sup>4</sup> The same conclusion can be arrived at from the coincidence in energy of the  $3d^9 4f^1$  state in the metal and in  $\text{LaF}_3$  and  $\text{La}_2\text{O}_3$ . In fact, the energy of an excitonic state may be different in the metal and an insulating compound.

From a more general point of view, we deduce that the  $3d^9 4f^{m+1}$  states formed in lanthanum and the rare earths can be deexcited through all the atomic transitions possible in an x-ray state, i.e., an ionized state with an inner-shell vacancy.

(c) The interactions between the  $\text{La}^{3+} 3d^9 4f^1$  highly excited states and the  $\text{La}^{4+}$ -ion continua are weak; it is the same for the autoionization transitions, which here, are of the type  $3d^9 4f^1 \rightarrow X^{-1}$ .

Indeed, for  $3d_{5/2}^{-1} 4f^1 (\frac{5}{2}, \frac{7}{2})$ , the energetically possible autoionization transitions take place to the continuum states of the  $\text{La}^{4+} (X^{-1})$  ion with  $X=4s, 4p, \dots$ . The interactions between the excited state and these continua are very weak because the energy of the excited state is much larger than the ionization energy of the subshells. This is in agreement with the fact that the  $(\frac{5}{2}, \frac{7}{2})$  absorption and emission lines are identical and well described by Lorentzian curves. Let us note that analogous results are expected for the excited states with an inner hole over the entire x-ray range.<sup>47</sup>

For  $3d_{3/2}^{-1} 4f^1 (\frac{3}{2}, \frac{5}{2})$ , the autoionization to  $3d_{5/2}^{-1} \epsilon l$  is energetically possible, but we have seen that the continuum of states associated with the  $3d_{5/2}$  subshell is very weak in the energy range of the  $(\frac{3}{2}, \frac{5}{2})$  discrete state. Thus the mixing of this discrete state with the continua is very weak. In agreement with this conclusion, the  $(\frac{3}{2}, \frac{5}{2})$  emission and absorption lines coincide in energy, the emission is very well described by a Lorentzian curve, and the shapes of absorption and emission lines are identical on the low-energy side. Moreover, because the coupling between the discrete and continuum states is weak, we can admit to a first approximation that the transitions to these various states are additive and treat the  $3d_{3/2}$  photoabsorption as the sum of a transition to the noninteracting discrete  $(\frac{3}{2}, \frac{5}{2})$  state and transitions to the  $3d_{3/2}^{-1}$  continuum.

(d) There exists in the metal a weak interaction between the  $3d^9 4f^1$  discrete excited states and the extended states in the solid: We have seen in Sec. III that this interaction is energetically possible only in the metal and not in  $\text{LaF}_3$  and  $\text{La}_2\text{O}_3$ . On the other hand, the resonant and characteristic  $5p$ - $3d$  emissions, which take place in the excited

system, are less intense in the metal than in  $\text{LaF}_3$  and  $\text{La}_2\text{O}_3$ . The relative probability of creating the excited system by direct excitation being the same to within the experimental precision for the three materials, we deduce that the number of excited systems deexciting by radiative processes is smaller in the metal than in  $\text{LaF}_3$  and  $\text{La}_2\text{O}_3$ . Moreover, the  $5p_{3/2} 3d_{5/2}$  characteristic emission is observed in the  $\text{La}^{4+}$  ion for the metal and not for the compounds. These results suggest that the excited atoms of the metal can decay to the ion via an interaction between the discrete excited state and the solid continuum. This decay process can be assimilated to a "tunneling" effect.<sup>4</sup> It is simultaneously responsible for the intensity differences and the broadening of the emission and absorption lines in the metal with respect to  $\text{LaF}_3$  and  $\text{La}_2\text{O}_3$ . This tunneling process decreases the number of excited states and is in competition with the relaxation process. It must be remarked that these differences remain small. It follows that the perturbation due to the extended states is weak, in agreement with the fact that all the other spectral characters are the same in the metal and the compounds.

In summary, the  $\text{La}^{3+} 3d^9 4f^1$  excited states can be treated as quasiatomic states in the solid, practically noninteracting with the underlying continua. These  $\text{La}^{3+} 3d^9 4f^1$  highly excited states have a different behavior from those of optical excited states which autoionize very rapidly. Indeed, the lifetime of an inner hole (here,  $3d$ ) is much shorter than that of a hole in an optical level. Then the autoionization is a relatively slow process as compared to the other recombination processes towards an inner hole which predominate. As a consequence, the  $3d^9 4f^1$  monoexcited states behave rather as x-ray states, and the radiative and nonradiative transitions which take place in an ion with an inner-shell vacancy can take place from  $3d^9 4f^1$ . It is convenient to designate these transitions by means of the usual x-ray spectroscopy terminology.

We propose that this terminology should be kept for the transitions involving the excited  $4f$  electron in  $\text{La}^{3+}$ . According to our observations these transitions take place between quasiatomic discrete states for which the configuration interaction, particularly with the continuum states, may be disregarded. Thus their decay may be described by the Weisskopf-Wigner independent-particle model. According to this model, it is possible to assign the direct radiative decay processes of the  $3d^9 4f^1$  state, i.e., the resonant lines, to characteristic x-ray emissions. It is well known that all the radiative x-ray transitions can have associated nonradiative Auger transitions. Consequently, we assign the  $3d^9 4f^1 \rightarrow X^{-1}$  transitions to Auger-type, transitions which are the direct nonradiative decays associated with the resonant emissions. In the same way, the  $3d_{3/2}^{-1} 4f^1 \rightarrow 3d_{5/2}^{-1}$  transitions can be assigned to Coster-Kronig-type transitions, as already discussed in Ref. 32.

It must be emphasized that the results we obtain for  $\text{La}^{3+}$  are different from those obtained for the  $3d$ - $4f$  transitions of  $\text{Cs}^+$  in  $\text{CsCl}$ .<sup>48</sup> The  $3d$ - $4f$  resonant emissions in  $\text{Cs}^+$  have Breit-Wigner-Fano-type shapes, but here the  $4f$  empty levels lie high in the conduction band and are strongly mixed with the empty extended states.

### B. $3d^9 4f^2$ states

From the isochromat spectra we have shown that the precursor states of  $\text{La}^{3+}$   $R^e$  lines are discrete states. Indeed, only the formation of an intermediate bound state consisting of the incident scattered electron in a localized atomic level together with the excited electron can explain the very strong and narrow enhancement observed by using CIS.

We have determined the energy of formation of these intermediate states for  $\text{La}_2\text{O}_3$  and  $\text{LaF}_3$ , and, from energy considerations, have confirmed that they have the  $3d^9 4f^2$  configuration. It has been suggested<sup>15</sup> that the initial state of  $R^e$  lines should be  $3d^9 Y^{-1} 4f^{n+2} + e^-$  as a consequence of a shakeup excitation which occurs simultaneously with the excitation of one  $3d$  electron to the  $4f$  level by interaction with the incident electron. The energy and the creation probability of such an initial state can be different in the metal and the two compounds (cf. Sec. III). The emission lines being practically identical for the three materials, this indicates that the valence states are not involved in the  $R^e$  transitions.

The  $3d^9 4f^2$  state can relax simultaneously by photon emission and nonradiative transitions just as any discrete state with an inner hole. We have interpreted the enhancement of the  $R_V$  resonance line at the  $3d_{3/2}$  threshold to be due to the nonradiative decay of  $3d_{3/2}^{-1} 4f^2$  to  $3d_{5/2}^{-1} 4f^1$  state, i.e., by a Coster-Kronig-type transition. Moreover, as seen by electron-excited Auger-electron APS,<sup>12</sup> the precursor state of the  $R^e$  emissions can decay by an Auger-type process. The simultaneous observation of radiative and nonradiative decay processes from  $R^e$  precursor states confirms that the  $R^e$  emissions are of the characteristic radiation type.

Thus, in agreement with our previous suggestion,<sup>13</sup> we attribute the  $R^e$  emissions to resonant emissions in the presence of an extra  $4f$  electron. Such emissions are observed when incident electrons with a kinetic energy equal to the energy of formation of the  $3d^9 4f^2$  state interact with  $\text{La}^{3+}$ . As shown by CIS, these emissions are very intense at threshold and can be observed at relatively high incident energies. The probability of creating this  $3d^9 4f^2$  state depends on the slowing-down function of incident electrons in the target. To determine the variation of the  $R^e$  line intensity as a function of  $E_0$ , it is necessary to know this slowing-down function and to treat the collisional interaction for an unseparable system formed by the incident electron and  $\text{La}^{3+}$ . The intensity of  $R^e$  lines also depends on the radiative-recombination probability of this state to  $3d^{10} 4f^1$  as compared to other recombination-process probabilities. Comparing the intensity of the  $R$  and  $R^e$  emissions and their variation with incident energy is thus a difficult problem.

In summary, the  $R^e$  lines are resonant lines in an excited system having a slow electron trapped in the weak  $\langle r \rangle$   $4f$  subshell. From a general point of view, one expects that  $X^{-1} Y^{+1}$  and  $X^{-1} Y^{+2}$  states could be created by interaction with an electron beam whenever strongly localized empty levels  $Y$  are present in a material, and provided that the  $X$  levels have a proper symmetry consistent with the dipole excitation to the  $Y$  level.

### VIII. CONCLUSION

All the data support the interpretation that the resonant effects present in the  $\text{La } 3d$  EXES of  $\text{LaF}_3$  and  $\text{La}_2\text{O}_3$  arise from the radiative decay of discrete states,  $3d^9 4f^1$  and  $3d^9 4f^2$ , almost noninteracting with the underlying continua and populated by direct excitation of the inner subshell. We have shown that the various transitions possible from an x-ray state, i.e., an inner-shell-vacancy-ionized state, can take place from these excited states. As an example, a characteristic line emitted in the presence of a  $4f$  spectator electron in the  $3d_{5/2}^{-1} 4f^1$  excited state has been evidenced. On the other hand, we have emphasized that, in contrast with the  $d$ - $f$  resonant emissions for which only the  $J=1$  levels of the  $3d^9 4f^1$  configuration contribute, all the  $J$  levels of this configuration can contribute to characteristic emission and Auger- and Coster-Kronig-type transitions.

To a first approximation it is possible to neglect the coupling effects at the initial state of the radiative processes and to suppose that these processes are decoupled from the excitation process. However, strictly speaking, only a theoretical treatment which considers the excitation process and radiative and nonradiative decay processes from all the  $J$  levels on a unified basis can correctly describe the  $\text{La}^{3+} 3d^{-1}$  excited states.

The role of the solid-state effects in the decay of the various excited x-ray states has been brought out by means of the comparison between results for  $\text{La}$  metal and  $\text{LaF}_3$  and  $\text{La}_2\text{O}_3$ . This role is very small because the excited x-ray states have a relatively large probability to decay by filling the inner hole before they can undergo a tunneling process; this arises from the localization of the  $\text{La } 4f$  wave function within the centrifugal well of the attractive potential due to the  $3d$  inner hole, and confirms that the  $\text{La } 3d$  spectra in the solid can be treated in terms of a quasiautomatic model.

To conclude, we would like to emphasize that EXES together with CIS makes it possible to identify the various excited x-ray states created under electron impact and to investigate their dynamics on a time scale defined by the lifetime of the inner hole.

<sup>1</sup>C. Bonnelle and R. C. Karnatak, C. R. Acad. Sci. (Paris) **268**, 494 (1969); J. Phys. (Paris) Colloq. **32**, C4-230 (1971).

<sup>2</sup>P. Motais, thèse de troisième cycle, Université de Paris, 1978.

<sup>3</sup>A. Belhrmi-Belhassan, thèse de troisième cycle, Université de Paris, 1979.

<sup>4</sup>C. Bonnelle, *Advances in X-Ray Spectroscopy* (Pergamon, New York, 1982), Chap. 6.

<sup>5</sup>G. Crecelius, G. K. Wertheim, and D. N. E. Buchanan, Phys. Rev. B **18**, 6519 (1978).

<sup>6</sup>J. Kanski, in *Proceedings of the XVIth Rare Earth Conference*,

- City, June 1981 (unpublished).
- <sup>7</sup>R. J. Liefeld, A. F. Burr, and M. B. Chamberlain, *Phys. Rev. A* **9**, 316 (1974).
- <sup>8</sup>M. B. Chamberlain, A. F. Burr, and R. J. Liefeld, *Phys. Rev. A* **9**, 663 (1974).
- <sup>9</sup>R. J. Smith, M. Piacentini, J. L. Wolf, and D. W. Lynch, *Phys. Rev. B* **14**, 3419 (1976).
- <sup>10</sup>G. Wendin and K. Nuroh, *Phys. Rev. Lett.* **39**, 48 (1977); *Phys. Rev. B* **24**, 5533 (1981).
- <sup>11</sup>W. E. Harte and P. S. Szczepanck, *Phys. Rev. Lett.* **42**, 1172 (1979).
- <sup>12</sup>J. Kanski and P. O. Nilsson, *Phys. Rev. Lett.* **43**, 1185 (1979).
- <sup>13</sup>P. Motais, E. Belin, and C. Bonnelle, in *Proceedings of the International Conference on Inner-Shell and X-Ray Physics of Atoms and Solids, Stirling, 1980*, edited by D. J. Fabian *et al.* (Plenum, New York, 1981), p. 451.
- <sup>14</sup>K. Ulmer, *Z. Phys. B* **43**, 101 (1981).
- <sup>15</sup>J. Kanski and G. Wendin, *Phys. Rev. B* **24**, 4977 (1981).
- <sup>16</sup>J. A. D. Matthew, G. Strasser, and F. P. Netzer, *Phys. Rev. B* **27**, 5839 (1983).
- <sup>17</sup>C. Bonnelle, R. C. Karnatak, and J. Sugar, *Phys. Rev. A* **9**, 1920 (1974).
- <sup>18</sup>J. M. Mariot and R. C. Karnatak, *J. Phys. F* **4**, L223 (1974).
- <sup>19</sup>J. K. Lang, Y. Baer, and P. A. Cox, *Phys. Rev. Lett.* **42**, 74 (1979).
- <sup>20</sup>J. Kanski, P. O. Nilsson, and I. Curelaru, *J. Phys. F* **6**, 1073 (1976).
- <sup>21</sup>S. Bergwall and A. Nigavekar, *Phys. Kondens. Mater.* **10**, 107 (1969).
- <sup>22</sup>C. G. Olson, M. Piacentini, and D. W. Lynch, *Phys. Rev. B* **18**, 5740 (1978).
- <sup>23</sup>S. Sato, Y. Sukisaka, and T. Matsukawa, in *Proceedings of the IVth International Conference on Vacuum Ultraviolet Radiation Physics, Hamburg* (Pergamon, New York, 1974), p. 414.
- <sup>24</sup>H. Berthou, thèse de doctorat d'Etat, Université de Paris, 1976.
- <sup>25</sup>D. W. Fisher and W. L. Baun, *J. Appl. Phys.* **38**, 4830 (1967).
- <sup>26</sup>J. Sugar, *Phys. Rev. A* **6**, 1764 (1972).
- <sup>27</sup>C. Bonnelle, R. C. Karnatak, and N. Spector, *J. Phys. B* **10**, 795 (1977).
- <sup>28</sup>J. E. Hansen, *Phys. Scr.* **21**, 510 (1980).
- <sup>29</sup>A. Belhrmi-Belhassan, R. C. Karnatak, N. Spector, and C. Bonnelle, *Phys. Lett.* **82A**, 174 (1981).
- <sup>30</sup>We thank Dr. N. Spector who kindly put at our disposal his diagonalization and recoupling program and for helpful discussions.
- <sup>31</sup>T. M. Zimkina, V. A. Fomichev, S. A. Gribovskii, and I. I. Zhukova, *Fiz. Tverd. Tela (Leningrad)* **9**, 1447 (1967) [*Sov. Phys.—Solid State* **9**, 1128 (1967)].
- <sup>32</sup>P. Motais, E. Belin, and C. Bonnelle, *J. Phys. F* **11**, L169 (1981).
- <sup>33</sup>J. P. Connerade and R. C. Karnatak, *J. Phys. F* **11**, 1539 (1981).
- <sup>34</sup>C. Bonnelle, *Ann. Phys. (N.Y.)* **1**, 439 (1966).
- <sup>35</sup>We thank J. Brosse, who helped carry out these calculations.
- <sup>36</sup>C. Feldman, *Phys. Rev.* **117**, 455 (1960).
- <sup>37</sup>M. Campagna, G. K. Wertheim, and Y. Baer, in *Photoemission in Solids*, edited by L. Ley and M. Cardona (Springer, Berlin, 1979), Vol. II, p. 217.
- <sup>38</sup>J. A. Bearden and A. F. Burr, *Rev. Mod. Phys.* **19**, 125 (1967).
- <sup>39</sup>S. Sato, *J. Phys. Soc. Jpn.* **41**, 913 (1976).
- <sup>40</sup>R. C. Karnatak, and A. Belhrmi-Belhassan, in *Proceedings of the International Conference on Inner-Shell and X-Ray Physics of Atoms and Solids, Stirling, 1980*, Ref. 13, p. 753.
- <sup>41</sup>G. Dufour, thèse de doctorat d'Etat, Université de Paris, 1978.
- <sup>42</sup>G. Wendin, *Phys. Rev. Lett.* **53**, 724 (1984).
- <sup>43</sup>F. Riehle, dissertation, Kernforschungszentrum Karlsruhe, 1977. Recently, we have found these unpublished results, which are in good agreement with ours.
- <sup>44</sup>K. Ulmer, *Z. Phys. B* **43**, 95 (1981).
- <sup>45</sup>N. Spector and C. Bonnelle (unpublished results).
- <sup>46</sup>E. McGuire, *Phys. Rev. A* **5**, 1043 (1972).
- <sup>47</sup>M. H. Tuilier, D. Laporte, and J. M. Esteva, *Phys. Rev. A* **26**, 372 (1982).
- <sup>48</sup>P. Motais, E. Belin, and C. Bonnelle, *Phys. Rev. B* **25**, 5492 (1982).